

PHILOSOPHICAL
TRANSACTIONS A

rsta.royalsocietypublishing.org

Research



Article submitted to journal

Subject Areas:computational physics,
coarse-graining, fluid mechanics**Keywords:**molecular dynamics, lattice gas
method, lattice Boltzmann method,
coarse-graining**Author for correspondence:**Alexander J. Wagner
e-mail: alexander.wagner@ndsu.eduMolecular dynamics lattice
gas equilibrium distribution
function for Lennard-Jones
particlesAleksandra Pachalieva^{1,2} and Alexander J.
Wagner³¹Center for Nonlinear Studies, Los Alamos National
Laboratory, Los Alamos, NM 87545, USA²Department of Mechanical Engineering, Technical
University of Munich, 85748 Garching, Germany³Department of Physics, North Dakota State
University, Fargo, ND 58108, USA

The molecular dynamics lattice gas method maps a molecular dynamics simulation onto a lattice gas using a coarse-graining procedure. This is a novel fundamental approach to derive the lattice Boltzmann method by taking a Boltzmann average over the molecular dynamics lattice gas. A key property of the lattice Boltzmann method is the equilibrium distribution function, which was originally derived by assuming that the particle displacements in the molecular dynamics simulation are Boltzmann distributed. However, we recently discovered that a single Gaussian distribution function is not sufficient to describe the particle displacements in a broad transition regime between free particles and particles undergoing many collisions in one time step. In a recent publication, we proposed a Poisson weighted sum of Gaussians which shows better agreement with the molecular dynamics data. We derive an lattice Boltzmann equilibrium distribution function from the Poisson weighted sum of Gaussians model and compare it to a measured equilibrium distribution function from molecular dynamics data and to a equilibrium distribution function from a single Gaussian probability distribution function.

THE ROYAL SOCIETY
PUBLISHING

© The Authors. Published by the Royal Society under the terms of the Creative Commons Attribution License <http://creativecommons.org/licenses/by/4.0/>, which permits unrestricted use, provided the original author and source are credited.

1. Introduction

The molecular dynamics lattice gas (MDLG) method [15, 16] uses a coarse-graining procedure to establish a direct link between microscopic methods – in particular, molecular dynamics (MD) simulation, and mesoscale methods such as lattice gas (LG) [3, 6] and lattice Boltzmann methods (LBM) [8, 18]. The MDLG fully relies on MD data and as such it rigorously recovers the hydrodynamics of the underlying physical system, and can be used to verify the behavior and examine the properties of the LG or the LBM methods directly without using the standard kinetic theory approach. Aspects that can be examined include fluctuating [2, 5, 10, 20], thermal [7, 11], multi-phase and multi component systems [4, 8, 12, 19].

A key feature in the LBM is the equilibrium distribution function. The LBM equilibrium distribution was originally derived by analogy to the continuous Boltzmann equation, where the equilibrium distribution for the velocities is a Maxwell Boltzmann distribution. Similarly, the LBM moments of the discrete velocity distribution were matched, to the degree possible, with the velocity moments of the Maxwell Boltzmann distribution. In the alternative derivation of the LBM from MD, it was shown that these previously postulated equilibrium distributions are indeed (at least approximately) consistent with the MDLG approach for specific discretization combinations for lattice and time spacing.

In the original MDLG calculation of the equilibrium distribution by Parsa *et al.* [15] it was assumed that the particle displacements in the molecular dynamics simulation are also Boltzmann distributed. This assumption gave an adequate prediction of the global equilibrium distribution function of the lattice Boltzmann method. However, later on by examining a non-equilibrium system undergoing a shear flow, we noticed small deviations (up to 5%) from the analytically predicted equilibrium distribution function. These deviations were traced back to the prediction of the one-particle displacement distribution function. In Pachalieva *et al.* [13], we proposed a correction of the displacement distribution function, which shows that a dilute gas with area fraction of $\phi = 0.0784$ and temperature of 20 LJ is better approximated by a Poisson weighted sum of Gaussians (WSG) probability distribution function. This remains true for a purely ballistic and purely diffusive regimes (for very small or very large time steps respectively), where the Poisson WSG formulation is reduced to a single Gaussian. In the current publication, we derive the MDLG equilibrium distribution function from the Poisson WSG one-particle displacement function and compare it to a measured equilibrium distribution function from molecular dynamics (MD) simulation and to the single Gaussian equilibrium distribution function. Our findings show that the Poisson WSG approximates the measured equilibrium distribution function significantly better.

The rest of the paper is summarized as follows: In Section 2, we briefly describe the MDLG method and how to derive the equilibrium distribution assuming that the displacement distribution is given by a single Gaussian. We then show how the equilibrium distribution function is altered if the displacements are instead distributed according to a Poisson WSG one-particle displacement function. This is followed by a detailed description of the MD simulation setup used to obtain the MD data given in Section 3. In Section 4, we compare the equilibrium distribution function obtained from the previously suggested single Gaussian, the novel Poisson weighted sum of Gaussians and the one measured from MD data. Our analysis shows significant improvement of the equilibrium distribution function analytical prediction when the Poisson WSG model is used. Finally, we give a brief conclusion and suggestions for future work in Section 5.

2. Derivation of the MDLG equilibrium distribution function

In the MDLG analysis, we impose a lattice onto a MD simulation and track the migration of the particles from one lattice position to another with displacement v_i after a time step Δt . A schematic representation of the lattice is given in Fig. 2b where the numbers 0 to 24 represent the

i index of the occupation number of a D2Q25 velocity set. The MDLG occupation number is thus given by

$$n_i(x, t) = \sum_j \Delta_x[x_j(t)] \Delta_{x-v_i}[x_j(t - \Delta t)], \quad (2.1)$$

with the delta function $\Delta_x[x_j(t)] = 1$, if particle x is in the lattice cell at time t , and $\Delta_x[x_j(t)] = 0$, otherwise. Here, the $x_j(t)$ is the position of the j -th particle at time t . The MDLG evolution equation is derived as

$$n_i(x + v_i, t + \Delta t) = n_i(x, t) + \Xi_i, \quad (2.2)$$

where the lattice gas collision operator Ξ_i given by

$$\Xi_i = n_i(x + v_i, t + \Delta t) - n_i(x, t). \quad (2.3)$$

The molecular dynamics lattice Boltzmann (MDLB) distribution function is defined as a Boltzmann ensemble average of the MDLG occupation number n_i and it is given by

$$f_i = \langle n_i \rangle_{\text{neq}}. \quad (2.4)$$

By taking the non-equilibrium ensemble average of Eq. (2.2), we obtain the MDLB evolution equation

$$f_i(x + v_i, t + \Delta t) = f_i(x, t) + \Omega_i, \quad \text{with} \quad \Omega_i = \langle \Xi_i \rangle_{\text{neq}}, \quad (2.5)$$

where Ω_i is the MDLB collision operator. A key element of the LBM is the global equilibrium distribution function, which in MDLB context is defined as an average of the lattice gas densities n_i over the whole MD domain and all iterations of an equilibrium MD simulation. The MDLB equilibrium distribution function writes

$$\begin{aligned} f_i^{\text{eq}} &= \langle n_i \rangle_{\text{eq}} \\ &= \left\langle \sum_j \Delta_x[x_j(t)] \Delta_{x-v_i}[x_j(t - \Delta t)] \right\rangle_{\text{eq}} \\ &= M \int dx_1 \int d\delta x_1 P^{(1),\text{eq}}(x_1, \delta x_1) \Delta_x[x_1] \Delta_{x-v_i}[x_1 - \delta x_1], \end{aligned} \quad (2.6)$$

where M is the total number of particles and $P^{(1),\text{eq}}$ is the one-particle displacement distribution function in equilibrium. This allows us to obtain the equilibrium distribution function f_i^{eq} analytically from the one-particle displacements Probability Distribution Function (PDF). In the MDLB formulation, the equilibrium distribution function depends solely on the one-particle displacement distribution function. Thus, knowing $P^{(1),\text{eq}}$ is crucial in predicting the equilibrium distribution function.

(a) Single Gaussian distribution model

Initially, Parsa *et al.* [15] suggested that the one-particle distribution function is given by a single Gaussian in one-dimension ($d = 1$)

$$P_\alpha^G(\delta x) = \frac{1}{[2\pi\langle(\delta x_\alpha)^2\rangle]^{d/2}} \exp\left[-\frac{(\delta x_\alpha - u_\alpha \Delta t)^2}{2\langle(\delta x_\alpha)^2\rangle}\right], \quad (2.7)$$

with displacements δx_α and second order moment $\langle(\delta x_\alpha)^2\rangle$. The solution factorizes for higher dimensions and it is given by

$$P^G(\delta x) = \prod_{\alpha=1}^d P_\alpha^G(\delta x_\alpha). \quad (2.8)$$

From Eq. (2.6) the equilibrium distribution function can be written as

$$\frac{f_i^{\text{eq},G}}{\rho^{\text{eq}}} = \prod_{\alpha=1}^d f_{i,\alpha}^{\text{eq},G}, \quad (2.9)$$

where

$$f_{i,\alpha}^{\text{eq},\text{G}} = N \left(e^{-\frac{(u_{i,\alpha}-1)^2}{2a^2}} - 2e^{-\frac{u_{i,\alpha}^2}{2a^2}} + e^{-\frac{(u_{i,\alpha}+1)^2}{2a^2}} \right) \\ + \frac{u_{i,\alpha}-1}{2} \left[\text{erf} \left(\frac{u_{i,\alpha}-1}{a\sqrt{2}} \right) - \text{erf} \left(\frac{u_{i,\alpha}}{a\sqrt{2}} \right) \right] \\ + \frac{u_{i,\alpha}+1}{2} \left[\text{erf} \left(\frac{u_{i,\alpha}+1}{a\sqrt{2}} \right) - \text{erf} \left(\frac{u_{i,\alpha}}{a\sqrt{2}} \right) \right], \quad (2.10)$$

with

$$a^2 = \frac{\langle (\delta x_\alpha)^2 \rangle}{(\Delta x)^2}, \quad N = \frac{a}{\sqrt{2\pi}}, \quad u_{i,\alpha} = v_{i,\alpha} - u_\alpha. \quad (2.11)$$

For details regarding the derivation of the Gaussian equilibrium distribution function, please refer to [15].

Even though this formulation shows very good agreement with the measured equilibrium distribution function from MD simulations, under more careful investigation we found that there are discrepancies of about 5%. This means that the displacement distribution function cannot be fully captured by a single Gaussian and a more complex distribution function has to be applied.

(b) Poisson weighted sum of Gaussians model

In Pachalieva *et al.* [13], we have introduced a correction of the displacements PDF proposed by Parsa *et al.* [15] using a Poisson weighted sum of Gaussians (WSG) instead of a single Gaussian distribution function. The Poisson WSG is given by

$$P^{\text{WSG}}(\delta x) = \sum_{c=0}^{\infty} e^{-\lambda} \frac{\lambda^c}{c!} P^c(\delta x), \quad (2.12)$$

where the $P^c(\delta x)$ probability distribution function factorizes for higher dimensions as

$$P^c(\delta x) = \prod_{\alpha=1}^d P_\alpha^c(\delta x), \quad (2.13)$$

with α being a Cartesian coordinate index. $P_\alpha^c(\delta x)$ is given by

$$P_\alpha^c(\delta x) = \left[\frac{(\lambda+1)}{2\pi(c+1)\langle(\delta x_\alpha)^2\rangle} \right]^{d/2} \exp \left[-\frac{(\lambda+1)(\delta x_\alpha - u_\alpha \Delta t)^2}{2(c+1)\langle(\delta x_\alpha)^2\rangle} \right], \quad (2.14)$$

where δx_α is the displacement in one-dimension, $\langle(\delta x_\alpha)^2\rangle$ is the second-order moment, u_α is the velocity, c is the number of occurrences, and λ is the average number of collisions. Similar to Eq. (2.9), the equilibrium distribution function can be expressed as

$$\frac{f_i^{c,\text{eq}}}{\rho^{\text{eq}}} = \prod_{\alpha=1}^d f_{i,\alpha}^{c,\text{eq}}, \quad (2.15)$$

where ρ^{eq} is the mass density and $f_{i,\alpha}^{c,\text{eq}}$ in one-dimension is written as

$$f_{i,\alpha}^{c,\text{eq}} = \left\{ \frac{N_c}{2\sqrt{\pi}} \left(e^{-\frac{(u_{i,\alpha}-1)^2}{N_c^2}} - 2e^{-\frac{u_{i,\alpha}^2}{N_c^2}} + e^{-\frac{(u_{i,\alpha}+1)^2}{N_c^2}} \right) \right. \\ \left. + \frac{(u_{i,\alpha}-1)}{2} \left[\text{erf} \left(\frac{(u_{i,\alpha}-1)}{N_c} \right) - \text{erf} \left(\frac{u_{i,\alpha}}{N_c} \right) \right] \right. \\ \left. + \frac{(u_{i,\alpha}+1)}{2} \left[\text{erf} \left(\frac{(u_{i,\alpha}+1)}{N_c} \right) - \text{erf} \left(\frac{u_{i,\alpha}}{N_c} \right) \right] \right\}, \quad (2.16)$$

with

$$N_c = \sqrt{\frac{2a^2(c+1)}{\lambda + 1}}, \quad a^2 = \frac{\langle (\delta x_\alpha)^2 \rangle}{(\Delta x)^2}, \quad u_{i,\alpha} = v_{i,\alpha} - u_\alpha, \quad (2.17)$$

where the average number of collisions λ could be approximated using the velocity auto-correlation function. However, to reduce the error coming from the theoretical average number of collisions and to eliminate the second-order and the fourth-order moment errors, we match these moments to the corresponding ones measured directly from the MD simulations. Thus, we obtain the following two solutions for the average number of collisions

$$\lambda_{1,2} = \frac{-9\mu_2^2 \pm \sqrt{3[15\mu_2^4 - 4\mu_2^2\mu_4] + 2\mu_4}}{2[3\mu_2^2 - \mu_4]}, \quad (2.18)$$

where $\mu_2 = \langle (\delta x_\alpha)^2 \rangle$ and μ_4 are the second- and fourth-order displacement moments, respectively. In Pachalieva *et al.* [13], we show that λ_2 provides an optimal solution, which we use to derive the Poisson WSG equilibrium distribution function.

$$f_i^{\text{eq,WSG}} = \sum_{c=0}^{\infty} e^{-\lambda} \frac{\lambda^c}{c!} f_i^c. \quad (2.19)$$

To construct the Poisson WSG, we measured the second-order and fourth-order displacement moments from the MD simulations. For detailed derivation and discussion of the Poisson WSG displacement distribution function, please refer to Pachalieva *et al.* [13].

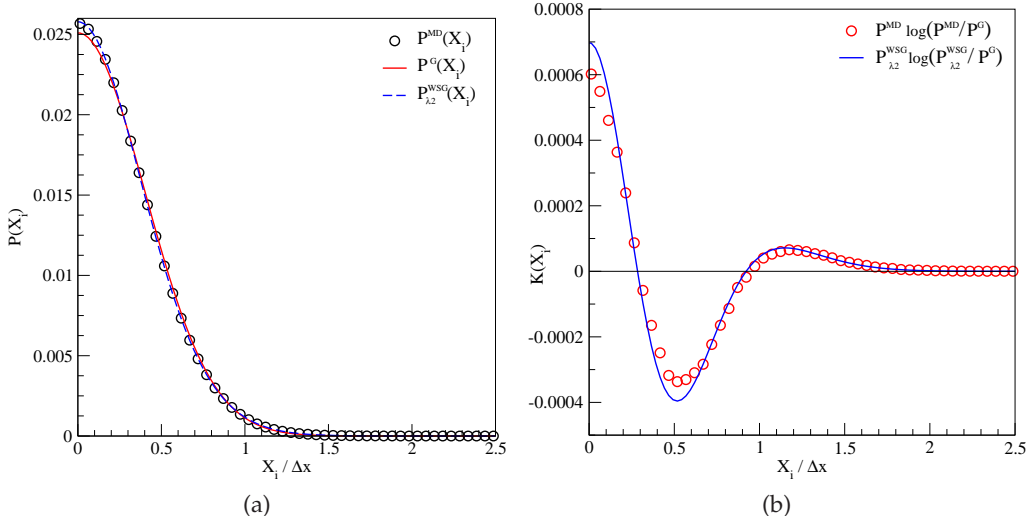


Figure 1. (Color online) (a) Displacements probability distribution functions. The symbols (black) depict a PDF obtained from an MD simulation of LJ particles in equilibrium. The line (red) illustrates a Gaussian probability distribution function defined in Eq. (2.7) with mean-squared displacement fitted directly to the MD data. The dashed line (blue) represents the Poisson WSG obtained from Eq. (2.12). Only the data for positive velocities has been depicted due to symmetry. (b) shows the difference between the distributions per interval X_i as defined in Eq. (2.20). The presented data is for the standard parameters used in the paper and a coarse-grained time step $\Delta t = 3.2$.

In Pachalieva *et al.* [13], we looked at the probability distribution function of the displacements and we measured precisely the deviations between the theoretical PDFs and the MD simulation data. Since these deviations are relatively small, we used the following function to quantify the

discrepancies

$$K(X_i) = K(R \parallel Q) = R(X_i) \log \left(\frac{R(X_i)}{Q(X_i)} \right), \quad (2.20)$$

where $R(X_i)$ and $Q(X_i)$ are probability distributions over an interval X_i . By performing a sum over all the bins X_i , we obtain the well known Kullback-Leibler (KL) divergence [9] defined as

$$D_{\text{KL}}(R \parallel Q) = \sum_i R(X_i) \log \left(\frac{R(X_i)}{Q(X_i)} \right). \quad (2.21)$$

The KL divergence measures the discrepancies of one probability distribution function to another. It is always non-negative $D_{\text{KL}}(R \parallel Q) \geq 0$ or equal to zero if and only if the probability distribution functions are identical $R(X_i) = Q(X_i)$ [9].

In Fig. 1a, we see the true probability distribution function obtained from the MD data $P^{\text{MD}}(X_i)$, the Gaussian probability distribution function $P^G(X_i)$, and the Poisson WSG distribution function $P^{\text{WSG}}(X_i)$. There is a visible divergence between the Gaussian and the other two distribution functions. We measured $K(X_i)$, as defined in Eq. (2.20), for $P^G(X_i)$ compared to the MD data and the Poisson WSG distribution function as shown in Fig. 1b. The results suggest that even though the Gaussian and the Poisson WSG probability distribution functions have the same second moment, their deviations in the higher moments influence strongly the form of the distribution function. In Section 4, we show how these deviations effect the LBM equilibrium distribution function.

3. Simulations setup

The measured equilibrium distribution function depicted as $f_i^{\text{eq,MD}}$ in Figs. 2a-4a is obtained from molecular dynamics simulations. To perform the MD simulations we used the open-source molecular dynamics framework LAMMPS [17, noa] developed by Sandia National Laboratories. The MD simulations consist of particles interacting with the standard 6-12 Lennard-Jones (LJ) intermolecular potential given by

$$V_{\text{LJ}} = 4\epsilon \left[\left(\frac{\sigma}{r} \right)^{12} - \left(\frac{\sigma}{r} \right)^6 \right], \quad (3.1)$$

with σ being the distance at which the inter-particle potential goes to zero, r is the distance between two particles, and ϵ is the potential well depth. The particle mass and the LJ particle diameter are set to $m = 1$ and $\sigma = 1$, respectively. The number of particles in each simulation has been fixed to $N = 99\,856$ which fills a two-dimensional (2D) square with length $L = 1000$ LJ units. The area fraction ϕ of the domain is calculated from the area of the circular LJ particles multiplied by the number of particles divided by the area of the domain, where the radius of the circular LJ particle is given by $\sigma/2$. The MD simulations considered in this publication have an area fraction of $\phi = 0.078387$. We initialised the simulations using homogeneously distributed particles with kinetic energy corresponding to 20 in LJ units. We focus our attention to MD simulations of a fairly dilute gas in equilibrium, since the assumption that the collision times is Poisson distributed is correct only for dilute systems.

The LJ timescale is given by the time needed for a particle with kinetic energy of half the potential energy well ϵ to traverse one diameter σ of an LJ particle. This can be also expressed as

$$\tau_{\text{LJ}} = \sqrt{\frac{m\sigma^2}{\epsilon}}. \quad (3.2)$$

The MD step size is set to 0.0001 τ_{LJ} which is considerably small to ensure high accuracy of the MD data. We define a dimensionless coarse-grained time step Δt being the product of the MD step size and the MD output frequency shown in Table 1. The time step Δt is chosen such that the MD simulations are restricted to the ratio of the mean-squared displacement and the squared

Table 1. MD simulation setup

Δt	Δx	lx	MD step size (τ_{LJ})	MD output frequency ($1/\tau_{\text{LJ}}$)	Number of iterations	Total MD time steps	Total MD time (τ_{LJ})
0.3911	4	250	0.0001	3 911	2 000	7 822 000	782.2
0.5000	5	200	0.0001	5 000	2 000	10 000 000	1 000.0
0.5626	5.5	180	0.0001	5 626	2 000	11 252 000	1 125.2
0.6927	6.6(6)	150	0.0001	6 927	2 000	13 854 000	1 385.4
0.9009	8.3(3)	120	0.0001	9 009	2 000	18 018 000	1 801.8
1.1261	10	100	0.0001	11 261	2 000	22 522 000	2 252.2
1.4994	12.5	80	0.0001	14 994	2 000	29 988 000	2 998.8
1.6342	13.3(3)	75	0.0001	16 342	2 000	32 684 000	3 268.4
2.0338	15.625	64	0.0001	20 338	2 000	40 676 000	4 067.6
2.9280	20	50	0.0001	29 280	2 000	58 560 000	5 856.0
4.1821	25	40	0.0001	41 821	2 000	83 642 000	8 364.2
6.1751	31.25	32	0.0001	61 751	2 000	123 502 000	12 350.2

lattice size being set to

$$a^2 = \frac{\langle (\delta x)^2 \rangle}{(\Delta x)^2} \approx 0.1611, \quad (3.3)$$

which corresponds to the parameter a^2 used in earlier publications [14, 15]. By fixing the value of a^2 to approximately 1/6, we ensure that most of the LJ particles in equilibrium will travel up to one lattice space which corresponds to an D2Q9 lattice Boltzmann method. To verify that the Poisson WSG equilibrium distribution function $f_i^{\text{eq},\text{WSG}}$ approximated the MD data better than the single Gaussian equilibrium distribution function $f_i^{\text{eq},\text{G}}$ across the length scale, from ballistic to diffusive regime, we vary the coarse-grained time step $\Delta t \in [0.3911, 6.1751]$ and the lattice size $\Delta x \in [4, 31.25]$ of the executed simulations. An overview of the MD simulation setup is given in Table 1. The number of lattice points lx varies from 250 to 32 depending on the coarse-grained time step Δt . For each coarse-grained time step Δt we performed 2 000 iterations which corresponds to total MD time of $782.2 \tau_{\text{LJ}}$ to $12 350.2 \tau_{\text{LJ}}$ for the smallest and largest coarse-grained time step Δt , respectively. In order to bring the molecular dynamics simulations to equilibrium state before we start collecting data, the initial 3 000 000 iterations of each simulation were discarded. The discarded iterations are not included in Table 1 for clarity.

The MD simulation setup characterizes a hot dilute gas in equilibrium with average velocity fixed to zero

$$Nu_\alpha = \sum_{j=1}^N v_{j,\alpha} = 0, \quad (3.4)$$

where N is the number of LJ particles.

We performed standard molecular dynamics simulations without thermostat. In the LAMMPS framework this is called NVE integration. The microcanonical ensamble NVE is characterized by constant number of particles (N), constant volume (V) and constant energy (E).

4. Results

In order to obtain a measured equilibrium distribution function, we post-process the collected MD data using the MDLG analysis tool. The MD domain is overlapped with a lattice and we trace the migration of the particles over time from one lattice to another. By doing this, we obtain the MDLG occupation numbers $n_i(x, t)$ as defined in Eq. (2.1) which after sufficient averaging deliver the MDLB equilibrium distribution function $f_i^{\text{eq},\text{MD}}$ as defined in Eq (2.6).

The analytical models of the equilibrium distribution function defined in Section 2 depend only on the choice of the one-particle displacement distribution function. Since we define two different one-particle distribution, we expect to see also changes in the respective equilibrium distribution function derived from them, even though their second-order moments are equivalent. However, a non-trivial question remains how the migration of particles from one node to another changes within a lattice.

To gain a better understanding, we calculate the equilibrium distribution function for an extended D2Q25 lattice which corresponds to two neighboring cells in X - and Y -directions for a two-dimensional domain. A schematic representation of the D2Q25 lattice is given in Fig. 2b. In equilibrium state with zero initial velocity, one distinguishes six sets of equilibrium distribution function contributions: $f_0^{\text{eq},*}$, $f_{1-4}^{\text{eq},*}$, $f_{5-8}^{\text{eq},*}$, $f_{9-12}^{\text{eq},*}$, $f_{13-20}^{\text{eq},*}$, and $f_{21-24}^{\text{eq},*}$, where each set has a unique displacement length from the central lattice. When measuring the equilibrium distribution function $f_i^{\text{eq,MD}}$ from the MD simulations, we average over the number of lattices for each set to obtain a symmetric probability distribution function. It is worth mentioning that the deviations of the $f_i^{\text{eq,MD}}$ values within each set are relatively small.

The MDLG analysis was introduced for an D2Q49 lattice including a third layer of neighbouring cells, however, the number of considered neighboring layers depends solely on the problem at hand. For a simulation in equilibrium with zero velocity, and a parameter a^2 as defined in Eq (3.3) being set to approximately 0.1611 we obtain an equilibrium distribution function $f_i^{\text{eq,MD}}$ for each lattice node.

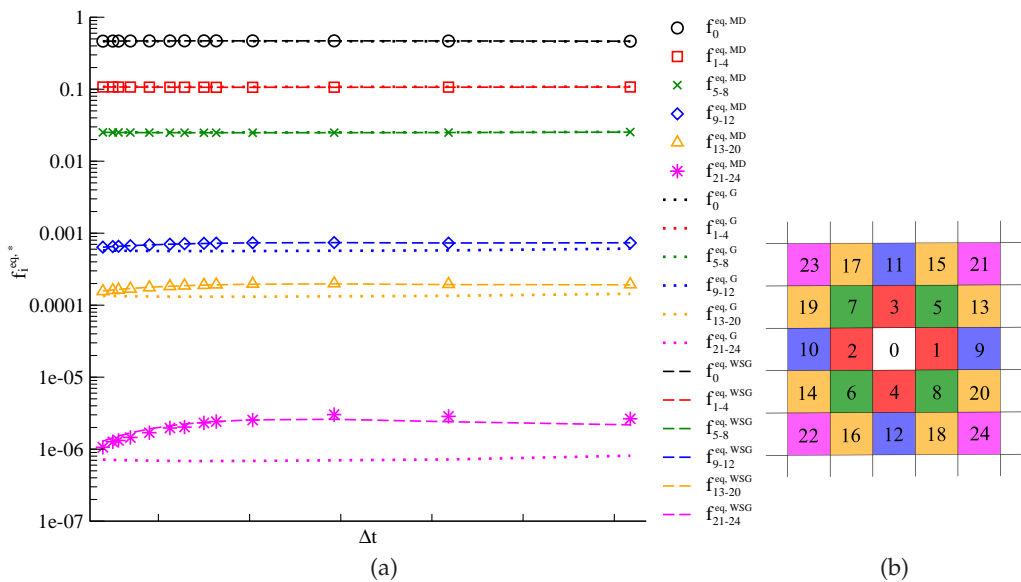


Figure 2. (Color online) (a) Estimated equilibrium distribution functions $f_i^{\text{eq},*}$ obtained either from MD simulation data ($f_i^{\text{eq,MD}}$), theoretical solution using a single Gaussian distribution function ($f_i^{\text{eq,G}}$) or theoretical solution using Poisson WSG ($f_i^{\text{eq,WSG}}$). (b) Schematic representation of the D2Q25 lattice. The equilibrium distribution function $f_i^{\text{eq},*}$ values are color coded and each color represents one of the six sets of equilibrium distribution function contributions. Here, the asterisk (*) corresponds to the variety of methods used to obtain an equilibrium distribution function: measured from MD simulation, single Gaussian analytical solution and Poisson WSG analytical solution.

The estimated equilibrium distribution function $f_i^{\text{eq},*}$ for a variety of coarse-grained time steps $\Delta t \in [0.3911, 6.1751]$ is shown in Fig. 2a. The equilibrium distribution function $f_i^{\text{eq},*}$, as

mentioned above, is obtained from three different methods: $f_i^{\text{eq,MD}}$ is measured from an MD simulation, $f_i^{\text{eq,G}}$ is theoretically estimated using a single Gaussian distribution function and $f_i^{\text{eq,WSG}}$ is theoretically estimated from a Poisson WSG distribution function. The theoretical equilibrium distribution function models are described in detail in Sections 2(a) and 2(b), respectively.

In Fig. 2a one can see that the largest equilibrium distribution function contributions are coming from the first layer neighbours $f_{0-8}^{\text{eq,*}}$. These nodes are approximated very well by both theoretical models, please refer to Fig. 3a for a detailed comparison of the measured and the theoretical $f_{0-8}^{\text{eq,*}}$. The next equilibrium distribution function groups $f_{9-12}^{\text{eq,*}}$ and $f_{13-20}^{\text{eq,*}}$ are significantly smaller than $f_{0-8}^{\text{eq,*}}$ with one to two order of magnitude. For $f_{9-12}^{\text{eq,*}}$ and $f_{13-20}^{\text{eq,*}}$, we see that the deviations of the measured and the theoretical single Gaussian model become larger. The Poisson WSG $f_{9-20}^{\text{eq,*}}$ show a very good agreement with the measured equilibrium distribution function. The diagonal nodes in the second layer $f_{21-25}^{\text{eq,*}}$ are even smaller and their value could be considered negligible. However, the measured equilibrium distribution function $f_i^{\text{eq,MD}}$ shows a good agreement with the theoretical Poisson WSG $f_i^{\text{eq,WSG}}$ even for very small contributions such as $f_{21-25}^{\text{eq,*}}$. This suggests that these contributions even though really small are not just noise b

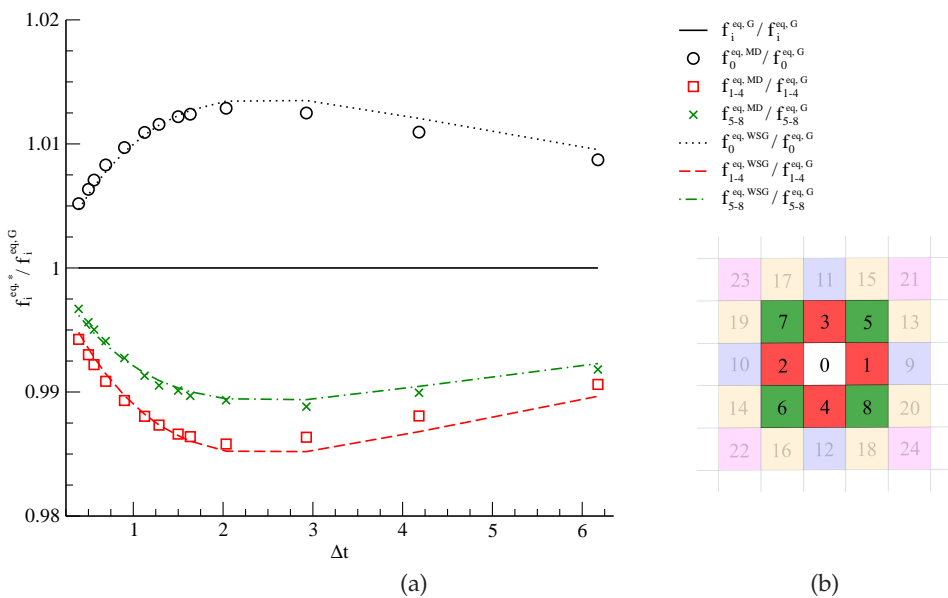


Figure 3. (Color online) (a) First layer equilibrium distribution functions $f_{0-8}^{\text{eq,*}}$ scaled to the Gaussian equilibrium distribution function. The equilibrium distribution functions are obtained either from MD simulation data ($f_{0-8}^{\text{eq,MD}}$), theoretical solution using a single Gaussian distribution function ($f_{0-8}^{\text{eq,G}}$) or theoretical solution using Poisson WSG ($f_{0-8}^{\text{eq,WSG}}$). (b) Schematic representation of the D2Q25 lattice. The equilibrium distribution function $f_i^{\text{eq,*}}$ values are color coded and each color represents one of the six sets of equilibrium distribution function contributions. Here, the asterisk (*) corresponds to the variety of methods used to obtain an equilibrium distribution function: measured from MD simulation, single Gaussian analytical solution and Poisson WSG analytical solution.

Figures 3a and 4a depict the equilibrium distribution functions scaled to the single Gaussian equilibrium function. They show how the measured from MD simulation and the novel Poisson WSG equilibrium distribution functions deviate from the single Gaussian. The first layer

equilibrium distribution function values are shown in Fig. 3a. These nodes have the largest contribution to the total equilibrium distribution function.

Fig. 3a shows more particles staying at node zero and a depression for the first neighbouring layer (nodes 1 to 8). This very same feature repeats itself in Fig. 1b. The $P_{\lambda 2}^{\text{WSG}} \log(P_{\lambda 2}^{\text{WSG}} / P^G)$ values depicted in blue show that the number of small displacements is enhanced $X_i / \Delta x \in [0, 1.6]$.

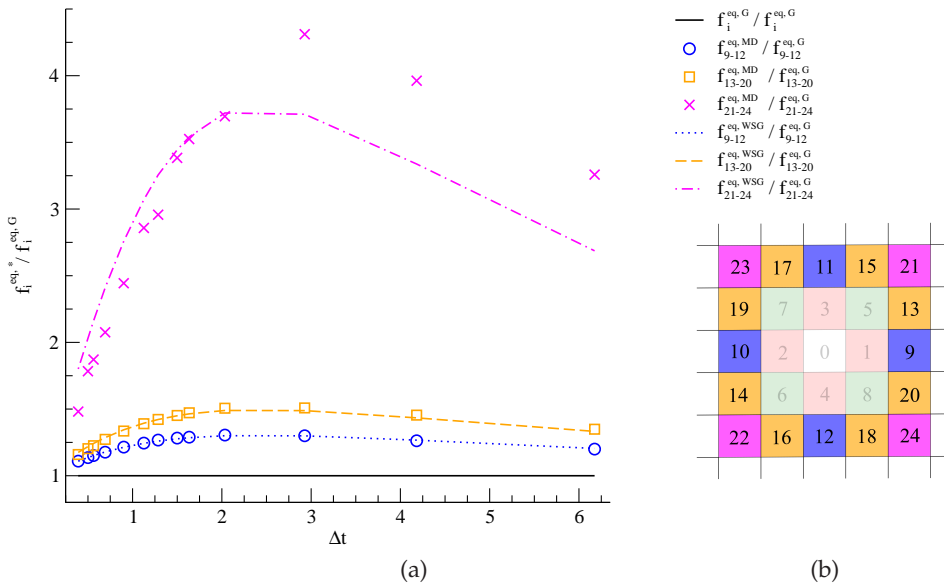


Figure 4. (Color online) (a) Second layer equilibrium distribution functions $f_{9-24}^{\text{eq},*}$ scaled to the Gaussian equilibrium distribution function. The equilibrium distribution functions are obtained either from MD simulation data ($f_{9-24}^{\text{eq,MD}}$), theoretical solution using a single Gaussian distribution function ($f_{9-24}^{\text{eq},G}$) or theoretical solution using Poisson WSG ($f_{9-24}^{\text{eq,WSG}}$). (b) Schematic representation of the D2Q25 lattice. The equilibrium distribution function $f_i^{\text{eq},*}$ values are color coded and each color represents one of the six sets of equilibrium distribution function contributions. Here, the asterisk (*) corresponds to the variety of methods used to obtain an equilibrium distribution function: measured from MD simulation, single Gaussian analytical solution and Poisson WSG analytical solution.

The second layer equilibrium distribution function values are depicted in Fig. 4a. In Fig. 1b we notice the enhanced probability of large displacements $X_i / \Delta x \in [0.9, 1.6]$ which corresponds to the larger values of $f_{9-24}^{\text{eq,WSG}}$ in Fig. 4a. The deviations (up to approx. 4.5%) from the theoretical single Gaussian equilibrium distribution function are also larger compared to the first layer nodes $f_{0-8}^{\text{eq,WSG}}$. Since the $f_{9-24}^{\text{eq,WSG}}$ true values are smaller by multiple orders of magnitude than the first layer neighbours $f_{0-8}^{\text{eq,WSG}}$ these deviations have a smaller impact on the total equilibrium distribution function, even though they are larger. Nevertheless, Fig. 4a shows clearly that the Poisson WSG equilibrium distribution function captures better the MD data.

5. Conclusion

In the pursuit of deriving a universal LBM collision operator, we investigated a non-equilibrium system where it is assumed that collisions keep the distribution functions close to local equilibrium, constrained by the conserved quantities, usually mass and momentum. This means

that even small errors in the formulation of the equilibrium distribution function influences the data obtained for the collision operator.

A key ingredient to predict the MDLB equilibrium distribution function correctly is the definition of the one-particle displacement distribution function. It is clear that even though the second-order moment of the single Gaussian and the Poisson WSG distribution function are the same, the derived equilibrium distribution functions show non-trivial behaviour which correlates with the raw probability distribution function. In conclusion, the Poisson WSG equilibrium distribution function captures better the measured equilibrium distribution function from MD data.

Data Accessibility. This manuscript has no further supporting data.

Authors' Contributions. AW supervised the research, contributed to it, and revised the manuscript. AP contributed to the research, embedded the proposed model, set up the test cases, performed the data analysis and wrote the manuscript. All authors read and approved the manuscript.

Competing Interests. The authors declare that they have no competing interests.

Funding. AP is partially supported by the Center for Nonlinear Studies (CNLS) and the Laboratory Directed Research and Development (LDRD) program at Los Alamos National Laboratory (LANL), and the German Federal Ministry of Education and Research (BMBF) in the scope of the project Aerotherm (reference numbers: 01IS16016A-B).

References

noa LAMMPS Official Website: <http://lammps.sandia.gov>.

- 2 Adhikari, R., Stratford, K., Cates, M. E., and Wagner, A. J. (2005). Fluctuating lattice boltzmann. *Europhysics Letters (EPL)*, 71(3):473–479.
- 3 Blommel, T. and Wagner, A. J. (2018). Integer lattice gas with Monte Carlo collision operator recovers the lattice Boltzmann method with Poisson-distributed fluctuations. *Physical Review E*, 97(2):023310.
- 4 Briant, A., Wagner, A., and Yeomans, J. (2004). Lattice boltzmann simulations of contact line motion. i. liquid-gas systems. *Physical Review E*, 69(3):031602.
- 5 Dünweg, B., Schiller, U. D., and Ladd, A. J. C. (2007). Statistical mechanics of the fluctuating lattice boltzmann equation. *Phys. Rev. E*, 76:036704.
- 6 Frisch, U., Hasslacher, B., and Pomeau, Y. (1986). Lattice-Gas Automata for the Navier-Stokes Equation. *Physical Review Letters*, 56(14):1505–1508.
- 7 He, X., Chen, S., and Doolen, G. D. (1998). A novel thermal model for the lattice boltzmann method in incompressible limit. *Journal of computational physics*, 146(1):282–300.
- 8 He, X. and Luo, L.-S. (1997). Theory of the lattice boltzmann method: From the boltzmann equation to the lattice boltzmann equation. *Physical Review E*, 56(6):6811.
- 9 Kullback, S. and Leibler, R. A. (1951). On information and sufficiency. *The annals of mathematical statistics*, 22(1):79–86.
- 10 Ladd, A. J. C. (1993). Short-time motion of colloidal particles: Numerical simulation via a fluctuating lattice-boltzmann equation. *Phys. Rev. Lett.*, 70:1339–1342.
- 11 McNamara, G. R., Garcia, A. L., and Alder, B. J. (1995). Stabilization of thermal lattice boltzmann models. *Journal of Statistical Physics*, 81(1-2):395–408.
- 12 Osborn, W., Orlandini, E., Swift, M. R., Yeomans, J., and Banavar, J. R. (1995). Lattice boltzmann study of hydrodynamic spinodal decomposition. *Physical review letters*, 75(22):4031.
- 13 Pachalieva, A. and Wagner, A. J. (2020). Non-Gaussian distribution of displacements for Lennard-Jones particles in equilibrium. *Phys. Rev. E*, 102:053310.
- 14 Parsa, M. R., Pachalieva, A., and Wagner, A. J. (2019). Validity of the molecular-dynamics-lattice-gas global equilibrium distribution function. *International Journal of Modern Physics C*, 30(10):1941007.
- 15 Parsa, M. R. and Wagner, A. J. (2017). Lattice gas with molecular dynamics collision operator. *Physical Review E*, 96(1):013314.
- 16 Parsa, M. R. and Wagner, A. J. (2020). Large fluctuations in nonideal coarse-grained systems. *Phys. Rev. Lett.*, 124:234501.

- 17 Plimpton, S. (1995). Fast Parallel Algorithms for Short-Range Molecular Dynamics. *Journal of Computational Physics*, 117(1):1–19.
- 18 Qian, Y. H., D'Humières, D., and Lallemand, P. (1992). Lattice BGK Models for Navier-Stokes Equation. *Europhysics Letters (EPL)*, 17(6):479–484.
- 19 Shan, X. and Doolen, G. (1995). Multicomponent lattice-boltzmann model with interparticle interaction. *Journal of Statistical Physics*, 81(1-2):379–393.
- 20 Wagner, A. J. and Strand, K. (2016). Fluctuating lattice boltzmann method for the diffusion equation. *Phys. Rev. E*, 94:033302.